International Journal of Automotive Technology, Vol. 6, No. 5, pp. 513–517 (2005)

1229–9138/2005/023–11

FATIGUE DURABILITY ASSESSMENT OF FULL-BEAD OF MLS GASKET USING FINITE ELEMENT ANALYSIS

S.-S. CHO[1], B. K. HAN[1]*, J.-H. LEE[1], H. CHANG[2] and B. K. KIM[3]

[1]Hongik University, Department of Mechanical & System Design Engineering, Seoul 121-791, Korea
[2]Hyundai Motor Company, 772-1 Jangduk-dong, Hwaseong-si, Gyeonggi 445-706, Korea
[3]Inje University, Department of Mechanical & Automotive Engineering, Gyeongnam 621-749, Korea

(Received 19 May 2004; Revised 9 July 2004)

ABSTRACT–A full-bead of multi-layer-steel engine head gasket, taking charge of the dynamic sealing of combustion chamber, is susceptible to fatigue failure. The fatigue durability of full-bead was assessed with the finite element analysis results and the high-cycle multi-axial fatigue theory. The assessment aimed to reveal the effects of the forming parameters and dimensions of full-bead. The results show that the selection of embossing parameters producing less deformation of bead plate is beneficial for the improvement of durability while the flatting has marginal influence. The fatigue durability also improves with the increase in the width of full-bead and the radial length of bore-side flat region. However, the dimensional effects are limited due to the occurrence of snap-through.

KEY WORDS : MLS cylinder head gasket, Full-bead, Fatigue durability, Finite element analysis, Sealing gap

1. INTRODUCTION

A cylinder head gasket is the component to seal the combustion gas, the lubricating oil and the coolant between the head and the block of internal combustion engines. Multi-layer-steel (MLS) gaskets are used in modern automotive engines because they correspond to a narrow land between cylinder bores, minimize the cylinder bore distortion and decrease the crevice volume as well as ensure high durability and reliability (Yamaguchi *et al.*, 1998) so that higher output and lighter weight of the engine can be accomplished simultaneously.

Figure 1 shows a schematic cross-sectional view of basic bead type MLS gasket. It is made of cold-rolled stainless steel with thin elastomer coatings on both sides for micro sealing. Beads, designating the embossed portions of plate, are compressed to be flat during the installation and recover their shape to maintain the contact with the head and the block when the head-block gap increases due to the combustion pressure. That is, the beads take charge of dynamic sealing. Full-beads are employed around the combustion chamber while half-beads are around the oil and coolant holes. Stopper, relatively thick portion around the engine bore, serves as the primary static sealing area. It also reduces the gap movement in the bead area by pretensioning the engine parts, and enhances durability of bead by limiting the bead deflection (Novak *et al.*, 1998). Shim plate, a separate narrow sheet contacting the full-bead, prevents leakage owing to surface porosity and diminishes wear in the bead area.

Since the gap between the head and the block varies periodically during the engine operation, the beads are subject to the periodic deformation and thus susceptible to fatigue failure. Hence, the fatigue durability is an essential requirement for the beads. The durability test in real engines during development has a lot of difficulties and may prolong the development period of engines. Hence, rig tests are conducted (Kestly *et al.*, 2000). Gasket is placed between two platens corresponding to the head and the block, and the gap is periodically varied to mimic the head-block interface. However, the rig test is time-consuming and provides only qualitative estimation because the gaskets are used in complicated circumstances (Ishigaki *et al.*, 1993). The alternative is a CAE approach using the finite element method. With the best knowledge of the authors, the only attempt is that of Popielas *et al.* (2000). Unfortunately the reliability of their assessment method cannot be assured with the results published.

This paper introduces an analytical assessment method for full-beads using the finite element analysis and the high-cycle multi-axial fatigue theory, and investigates the effects of forming parameters and dimensions of full-

*Corresponding author. e-mail: bkhan@wow.hongik.ac.kr

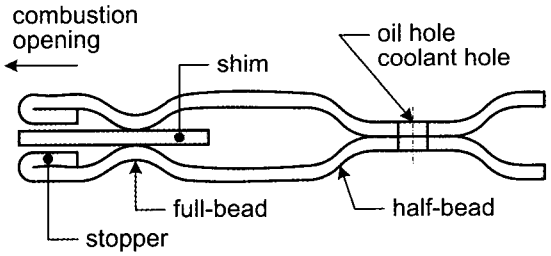

Figure 1. Basic structure of MLS bead type gasket.

beads on the durability.

2. FINITE ELEMENT ANALYSIS

Finite element analysis to obtain variation of stresses in the bead plate during the cyclic variation of head-block gap was performed with the model that were developed by the authors (Cho *et al.*, 2005). The model also simulates the bead forming process that consists of the embossing operation to form the full-bead and the flatting operation to adjust the bead height.

The mesh was constructed for the annular region of the gasket including the full-bead around the engine bore (refer to Figure 2). The bead plate consists of 0.2 mm thick stainless steel plate and two layers of 0.025 mm thick coatings. The cross-sectional width of the annular plate was 5.7 mm. The mesh was constructed with 4-node axisymmetric hybrid elements of 25 μm × 25 μm. The embossing punch and die, and the flatting dies for the simulation of forming process, and the cylinder head and block for the simulation of fastening and head lift-off were constructed with rigid bodies. Corner radius of the embossing dies was assumed to be 50 μm.

Stress-strain curves for both the stainless steel thin plate and the NBR were obtained from uniaxial tensile and compression tests. Based on these curves the plate was assumed as an elasto-plastic material with an elastic

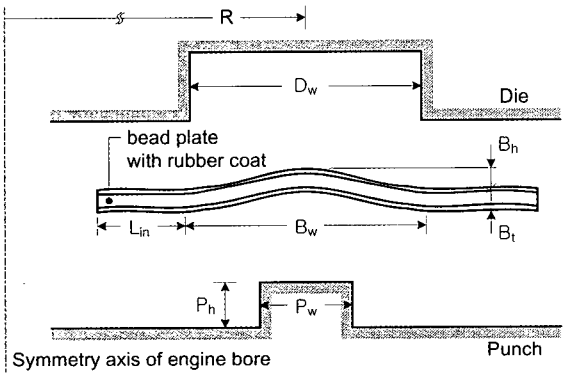

Figure 2. Schematic representation of full-bead, embossing punch and die with nomenclature.

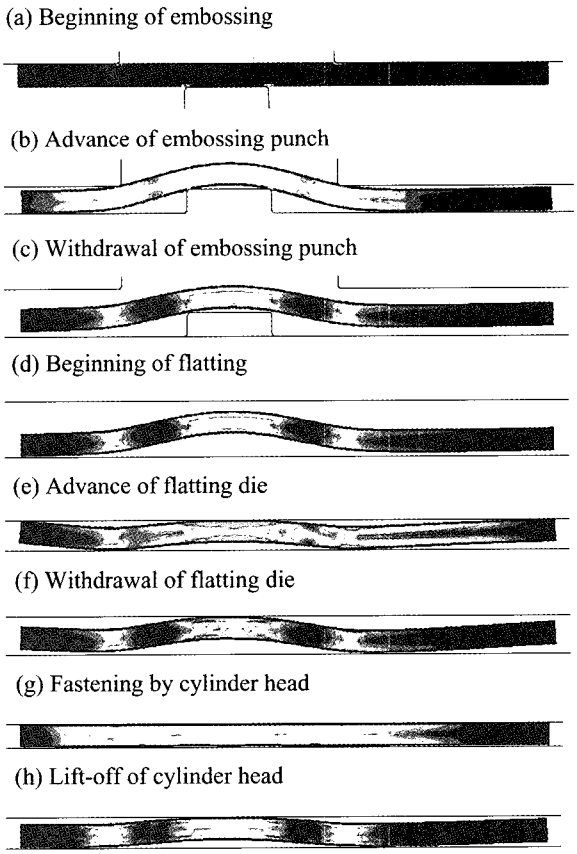

Figure 3. Finite element analysis procedure.

modulus of 185 GPa, a 0.2% off-set yield strength of 845 MPa, and an ultimate tensile strength of 1.4 GPa, while the NBR as a hyperelastic material with the strain energy potential U given by

$$U = \sum_{i=1}^{2} C_{i0}(\bar{I}_1 - 3)^i \tag{1}$$

where $C_{10} = 7.24$ MPa and $C_{20} = 8.90$ kPa, $\bar{I}_1$ is the first deviatoric strain invariant. Friction coefficient of the NBR-coated bead plate against the head and block was set equal to 0.2 because sliding friction tests of the NBR-coated stainless steel plate against the steel block gave the friction coefficient in the range from 0.1 to 0.3.

The simulation was conducted with a commercial finite element code ABAQUS. A quasi-static incremental solution technique was employed with nonlinear geometry analysis scheme. Figure 3 shows an analysis procedure. The analysis starts with the forming simulation of full-bead. The full-bead is embossed with a set of punch and die (Figure 3(a)–(c)). Since the embossed full-bead is taller than the height specified in the design, the flatting operation (Figure 3(d)–(f)) follows to adjust the height. After the forming is completed, the full-bead is fastened between the cylinder head and the block by moving down

the head (Figure 3(g)). After the full-bead is installed, the cylinder head moves upward to simulate the lift-off of the head during which the full-bead recovers its shape (Figure 3(h)). The up-and-down movement is repeated five times to stabilize the recovery behavior of bead, and then variation of stresses in the bead plate with the head lift-off is obtained for fatigue analysis.

3. FATIGUE ANALYSIS

The stress amplitude versus life (S-N) curve approach in the high-cycle multi-axial fatigue theory is used in this analysis because the full-bead is deformed elastically in a multi-axial stress state during the compression and recovery. Since the variation of uniaxial compressive fastening load generates stress amplitude in the full-bead that exhibits marginal difference in the direction of principal stresses, Sines' theory (Fuchs *et al.*, 1980) in the muti-axial fatigue theories is used where the equivalent stress amplitude S_{qa} is given by

$$S_{qa} = \sqrt{\frac{(S_{a1}-S_{a2})^2 + (S_{a2}-S_{a3})^2 + (S_{a3}-S_{a1})^2}{2}} \quad (2)$$

where S_{a1}, S_{a2} and S_{a3} are principal stress amplitudes.

Fatigue tests were conducted to obtain the S-N curve for the full-bead. In the test the full-bead was compressed and released repetitively between two platens for a given compressive load range. The load ranges were selected based on the practical fastening load. Since the nucleation of fatigue crack is difficult to detect during the test, the full-bead was compressed repetitively for the given number of cycles, and then examined with an optical microscope and a scanning electron microscope to identify the generation of fatigue cracks. Figure 4 shows the fatigue test redults and an approximate S-N curve. The stress amplitudes generated by the load ranges in the tests were calculated with the finite element analyses for the full-bead fatigue tests. The endurance limit, Se exists between 250 MPa and 350 MPa so that *Se*=300 MPa is

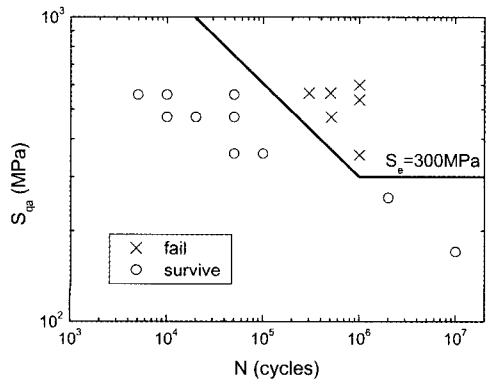

Figure 4. Fatigue life of full-bead.

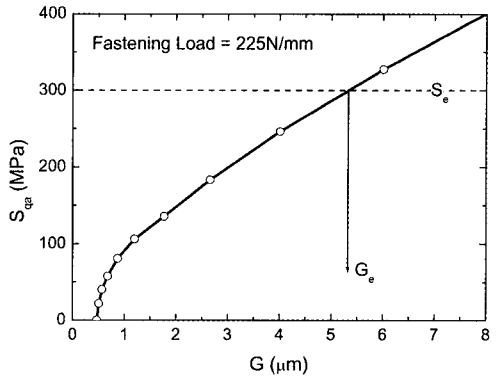

Figure 5. Variation of stress amplitude in the full-bead with sealing gap.

assumed in this study. The effect of mean stress on the endurance limit is disregarded because the uniaxial fatigue tests with standard thin plate specimen revealed marginal influence of mean stress on the endurance limit in the practical stress range of full-bead (Han *et al.*, 2004). It is noted that the approximate estimation of Se is sufficient for the present study because the effect of forming parameters and dimensions of full-bead on the fatigue durability is aimed in this study.

Figure 5 shows the magnitude of stress amplitude as a function of the sealing gap at the head-block interface (called the S-G curve hereafter) that is obtained from the finite element analysis. The magnitude of the stress amplitude is the maximum value of the stress amplitude in the full-bead, i.e., the stress amplitude at the weakest point. The sealing gap is defined as the head-block gap substracted with the thickness of the bead plate B_t. The stress amplitude increases with the gap, implying that the full-bead is cracked at the fewer number of cycles when the lift-off of the head is larger. When the gap is approximately 5.6 mm, the maximum stress amplitude reaches the endurance limit of 300 MPa. The gap producing the stress amplitude of the endurance limit is the maximum allowable gap for infinite life, G_e. The fatigue durability of full-bead is assessed with the value of G_e because the gap data are readily available from finite element analyses or experiements for the cylinder head-block compounds. It is noted that larger G_e means better durability of full-bead.

4. RESULTS AND DISCUSSION

4.1. Forming Parameters

Figures 6–8 show the dependence of the maximum allowable sealing gap for infinite life G_e on the embossing parameters, i.e., the punch-die clearance C_p at the end of embossing stroke, the height P_h and width P_w of the embossing punch, respecively. The embossing parameters

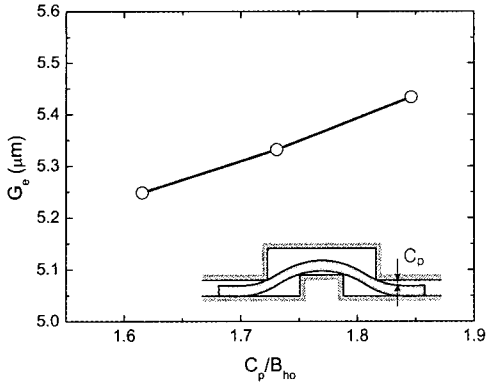

Figure 6. Effect of punch –die clearance at the end of embossing stroke.

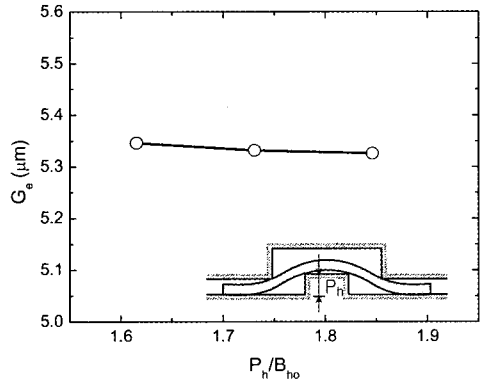

Figure 7. Effect of embossing punch height.

are normalized with the height of full-bead before the installation. Recalling that larger G_e means better durability, the fatigue durability improves with the increase in the clearance (Figure 6), with the decrease in the punch height (Figure 7), and with the decrease in the punch width (Figure 8). The increase in the clearance and the decrease in the height and width of punch result in

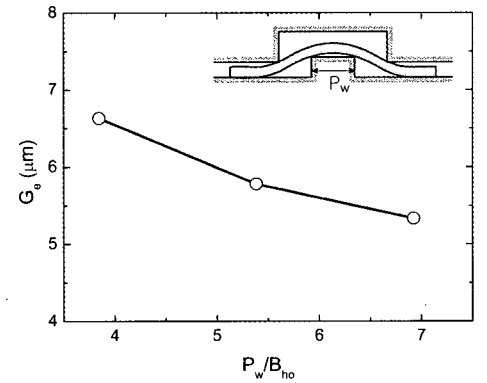

Figure 8. Effect of embossing punch width.

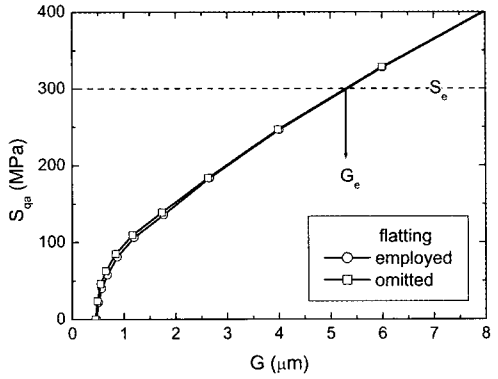

Figure 9. Effect of flatting operation.

smaller bending angle at the corners of the full-bead that are in contact with the corners of the die, and thus less deformation. Hence, it is concluded that the fatigue durability can be enhanced if the embossing parameters are selected to reduce the deformation in the bead plate. Since the embossing parameters were varied in practically acceptable ranges, it is claimed that the punch width is the most influencing parameter, the clearance is the secondary one, and the punch height is the negligible one.

Figure 9 shows the S-G curves where the flatting operation is conducted in one case while it is not in the other after the full-bead is embossed under an identical condition. The marginal difference is observed only when the sealing gap is smaller than 3 μm. Hence, it is considered that the flatting operation has marginal influence on the fatigue durability of the full-bead.

4.2. Dimensions of Full-bead

Figure 10 shows the effect of full-bead width. In order to consider only the influence of full-bead width, the widths of embossing punch and die cavity were varied in proportion to the bead width such that the horizontal clearance between the punch and the die remains

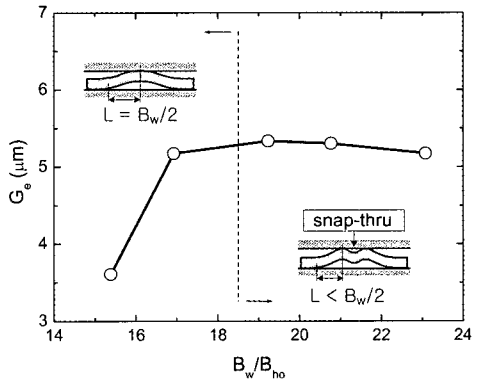

Figure 10. Effect of full-bead width.

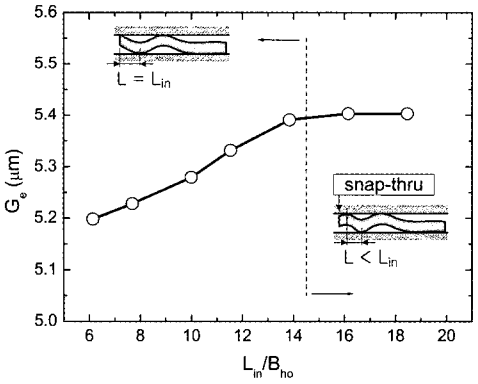

Figure 11. Effect of radial length of bore-side flat region of full-bead.

unaltered. The maximum allowable gap for infinite life G_e increases with the bead width until $B_w/B_{ho} = 19$, and then decreases, implying the optimal width exists. When the sealing gap is the same, the stress amplitude in the full-bead increases with the decrease in the horizontal distance between the contact points of the full-bead with the head and the block (the distance shown in the sub-figures of Figure 10). Since the distance between the contact points increases with the width of full-bead, the wide full-bead is subject to the smaller stress amplitude at the same sealing gap than the narrow full-bead, and thus G_e increases with the width of full-bead. However, when the full-bead width is very large (for $B_w/B_{ho} > 19$ in the present study), the sanp-through occurs at the top of the full-bead in contact with the head (refer to the sub-figure in Figure 10). As a result, the distance between the contact points is reduced and thus G_e decreases with the width of full-bead. Therefore, it is concluded that the fatigue durability improves with the increase in the width of full-bead unless the snap-through occurs.

Figure 11 shows the effect of radial length of bore-side flat region. The G_e increases with the radial length of bore-side flat region until the length L_{in}/B_{ho} reaches approximately 15, and then G_e levels off. The length of flat region increases the distance between the contact points (refer to the sub-figure in Figure 11) and thus the G_e as explained in the effect of full-bead width. The level-off is also attributed to the occurrence of the snap-through of the inner part of the flat region. Therefore, it is summarized that the fatigue durability improves with the increase in the radial length of the bore-side flat region unless the snap-through occurs.

5. CONCLUSION

Fatigue durability of full-bead of MLS cylinder head gasket was assessed using the finite element analysis and the high-cycle multi-axial fatigue theory. The assessment aimed to reveal the effects of forming parameters and dimensions of the full-beads.

The embossing process has the effect on the fatigue durability while the flatting process does not. During the embossing process, the selection of parameters generating the less deformation of bead plate such as the increase in the punch-die clearance at the end of embossing stroke and the decrease in the height and width of the embossing punch is beneficial for the improvement of the fatigue durability. The most significant parameter is the punch width.

With the increase in the width of full-bead and the radial length of the bore-side flat region, the fatigue durability of full-bead improves because of the increase in the distances between the contact points of full-bead with the head and the block. However, when the width of full-bead or the radial length of flat region is very large, the fatigue durability is no further enhanced or even reduced because the snap-through occurs at the top of the full-bead or the inner part of the flat region so that the distances between the contact points do not increase any more or even decrease.

REFERENCES

Cho, S.-S., Han, B. K., Chang, H. and Kim, B. K. (2005). Effect of forming process on sealing performance of full-bead of MLS gasket – finite element analysis approach. *Int. J. Automotive Technology* **6**, **2**, 191–196.

Fuchs, H. O. and Stephens, R. I. (1980). *Metal Fatigue in Engineering.* John Wiley & Sons. New York. 176–181.

Han, B. K., Cho, S.-S., Chang, H. and Kim, B. K. (2004). Fatigue fracture of NBR-coated SUS301 thin plate for MLS gasket. *Trans. Korean Society Automotive Engineers* **12**, **4**, 207–212.

Kestly, M., Popielas, F., Grafl, D. and Weiss, A. (2000). Accelerated testing of multi-layer steel cylinder head gaskets. *SAE Paper No.* 2000-01-1188.

Ishigaki, T., Kitagawa, J. and Tanaka, A. (1993). New evaluation method of metal head gasket. *SAE Paper No.* 930122.

Novak, G., Sadowski, M., Widder, E. and Capretta, R. (1998). The role of the stopper in the mechanics of combustion seals. *SAE Paper No.* 980575, 1–6.

Popielas, F., Chen, C. and Obermaiser, S. (2000). CAE approach for multi-layer-steel cylinder head gaskets. *SAE Paper No.* 2000-01-1348.

Yamaguchi, K., Sato, A., Goto, E., Fujiki, R., Kawai, Y. and Nakata, N. (1998). Development of a new metal cylinder head gasket. *SAE Paper No.* 980844, 1334–1338.